11th International Workshop on Ship and Marine Hydrodynamics
Hamburg, Germany, September 22-25, 2019

NUMERICAL AND TEST ANALYSIS FOR SELF-PROPULSION PERFORMANCE OF A TRAILING SUCTION HOPPER DREDGER

Zhigao Luo[1], Long Yu[1,2,3,*]

[1]State Key Laboratory of Ocean Engineering, Shanghai Jiaotong University, Shanghai 200240, China
[2]Collaborative Innovation Center for Advanced Ship and Deep-Sea Exploration(CISSE), Shanghai 200240, P.R. China.
[3]School of Naval Architecture, Ocean & Civil Engineering, Shanghai Jiaotong University, Shanghai 200240, China

*Corresponding author: Long Yu , yulone@sjtu.edu.cn

ABSTRACT

Resistance and self-propulsion performances of trailing suction hopper dredger (TSHD) remains a hot issue in predicting and improving performances of TSHD. In this paper, the CFD simulation technology and overset technology are used to calculate the resistance performance of TSHD at different velocities, and the results are accord with the model test results. Then overset technology is used to calculate the self-propelled performances of THSD equipped with different propellers under different working conditions. The results are consistent with the tests results. The performances between two kinds of propellers are compared and analyzed through field analysis.

1 INTRODUCTION

The hull of trailing suction hopper dredger (TSHD) is relatively large, and its resistance and self-propulsion performances are different under different working conditions. TSHD has the functions of dredging and loading, self-propelled transportation, bottom opening and discharging, dredging and shore discharging, and bow spraying. It is widely used in waterway and port dredging, infrastructure construction, urban human settlements and energy engineering, and plays an important role in dredging fleet. The Chinese dredging companies have been focusing on flexibility and developing multi-task TSHD, which will also improve the cost and consumption [1].

With the development of social economy, green shipbuilding has become an important requirement for the development of shipbuilding industry. As an engineering ship, the TSHD is developing towards large-scale and intelligent. The emissions and fuel consumptions of TSHD becomes larger recent years [2]. With the rise of international oil price and the development of ship form itself, it is of great significance to save energy and reduce emissions. With the development of CFD technology, it's feasible to utilize computer to analyze the resistance and self-propulsion performance of the ships and to modify the molded line or design energy-saved rudders and propellers [3]. Topics to predict resistance and self-propulsion performances emerge and advance rapidly in recent years.

Jeong Hwa Seo applied sliding mesh technique to facilitate to facilitate the rotating propeller for propeller open-water test and self-propulsion test. The results accord with the experiment results well. And the efficiency is lower than experiment results and other numerical results, which may be caused by the diffusion of the meshing [4]. Caricca used dynamic overset grids and hierarchy of bodies to allow the deflection of rudders while simulating turn and zigzag maneuvers. The results agree with tests well and indicate that the method is feasible. In his study, body force is used to simulate propeller rotating, which can not represent motions and influence of propellers adequately [5]. Then Carrica also used overset grids to simulate zigzag experiments of KCS. The results is good enough to predict the performances of hull and propeller. Meshes around rudder is not good enough to capture the flow. And the computing costs is high [6]. Nobuaki Sakamoto and Carrica validate results of forces and moment coefficients, hydrodynamic derivatives, and reconstructions of forces and moment coefficients from resultant hydrodynamic derivatives for a surface combatant Model 5415 bare

hull under static and dynamic planar motion mechanism simulations. Grids and time step convergence are proved to be reliable [7]. Dario show that hydrostatic particulars for intermediate loading conditions of variable ship geometry can be calculated by using analytical solutions of basic hydrostatic integrals [8].

Nowadays, how to promote the performances of TSHD through improving the molded lines, propellers and rudders is still a key issue. In this passage, the resistance performances under various speed and self-propulsion performances under 2 common working conditions are computed. 2 propellers are applied to the TSHD to verify the reliability of CFD and overset method. And the cause of the performance differences between 2 propellers are analyzed and the various fields conducted by the propellers are discussed.

2 NUMERICAL METHOD

The governing equations for the mass and momentum are shown as formula (1), formula (2):

$$\nabla \cdot V = 0 \tag{1}$$

$$\frac{\partial u}{\partial t} + div(u\boldsymbol{V}) = -\frac{1}{\rho}\frac{\partial p}{\partial x} + vdiv(grad\ u) \tag{2}$$

To capture the character of the wave, VOF (volume of fluid) is utilized. Free-surface waves behind hulls with different propellers distinct from different style and different velocity. And the wake and waves produced by propellers will react on the hull and rudders, changing resistance performance and self-propulsion performances.

STAR-CCM+, the CFD software, is used to carry out all the cases discussed in the passage. Unstructured grids are employed to build background grids and overset grids.

3 EXPERIMNTAL CONDITIONS

The tests are executed for TSHD resistance performance and self-propulsion performance. The tests are performed in the towing tank which is 110m in length, 6m in width and 3m depth. TSHD shown in Fig.1 is adopted for both experiments and numerical simulation. The main particulars of the TSHD are shown in Table.1 :

Table 1: main particulars of the TSHD

Main particular		ship	model
Scale ratio	[-]	1:1	1:28.46
L_{pp}(m)	[m]	120.00	4.216
B(m)	[m]	18.40	0.646
T(m)	[m]	6.80	0.239
$\nabla(m^3)$	[m^3]	11842.70	0.514
S(m^2)	[m^2]	3170.00	3.913

Figure 1: model and numerical TSHD model

In this paper, the distinct of self-propulsion performance between 2 types of propellers will be studied. The original propeller and the new designed propeller which is a ducted-propeller are shown in Fig.2. The particulars of 2 propellers are shown in Table.2:

Table 2:main particulars of 2 types of propellers

Main particular		Original propeller		Ducted-propeller	
		Ship	Model	Ship	Model
D	[mm]	3700	130	3200	112.4
Scale ratio	[-]	1:1	1:28.46	1:1	1:28.46
P/D	[-]	0.438	0.640	0.78	0.80
A_e/A_0	[-]	0.707	1.099	0.55	0.55
No. of blades	[-]	4		4	
Type	[-]	FP		HR	
Rotation	[-]	Right hand		Right hand	

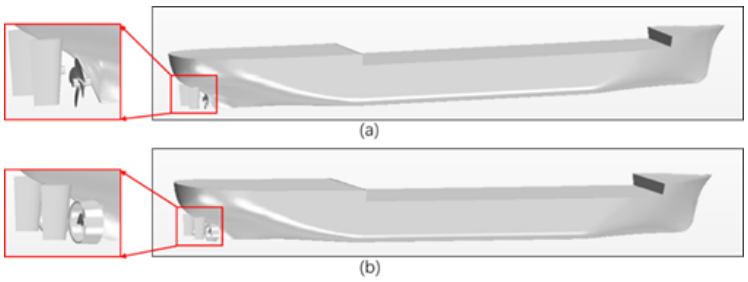

Figure 2: model/numerical propeller models

4 MODEL, GRIDS AND CONDITIONS

4.1 MODEL AND GRIDS

In order to match the experiment condition, the computational domain is set as a virtual towing tank whose length is 20m, about 4 times of the length of the ship, width is 12m, about 3 times of the width of the ship.

When studying the TSHD's static resistance performance at various speeds, rudders and hull are prepared both experiments and simulation, without propeller. Hence, only background grids and oversets around rudders are needed (Fig.3).

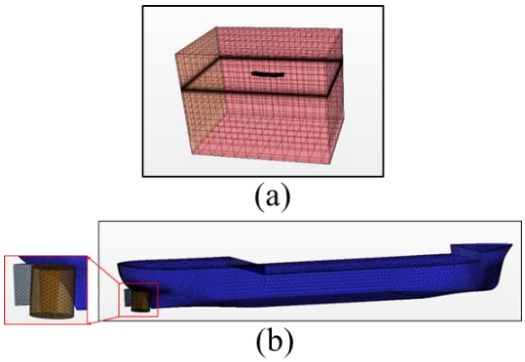

Figure 3: (a) Background regions
(b) oversets around rudders

When studying the TSHD's self-propulsion performance at different, hull, rudders and propellers are all prepared for simulations. Hence, only background grids, oversets around rudders and oversets around the propellers are needed. Background grids oversets around the rudders are the same as in static resistance simulations. Because of the difference between the 2 types of propellers, the oversets are established differently, as shown in Fig.4.

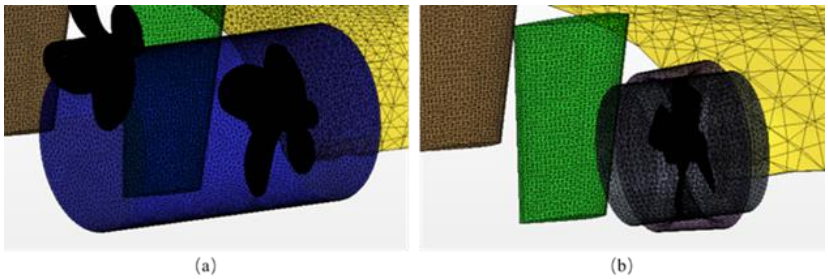

Figure 4: oversets around propeller models: (a) original propeller
(b) ducted-propeller

Table.3 cases under various working conditions, grids regions and grids number.

Parts	Rudder	Background	Original propeller	Ducted-propeller
Grid number	172159	1158781	705467	830299
Resistance simulation	1	1	0	0
Self-propulsion with original propeller	1	1	1	0
Self-propulsion with ducted-propeller	1	1	0	1

Grid independence will be discussed in the following part, which decides the density of the grids. 1 represents used, 0 represents unused.

4.2 CONDITIONS

Computing regions are set as the towing tank in width. The depth is 9m which can eliminate the effect of shallow water, and the velocity inlet is about 2 LPP distant from the stern, which lets the stream in at the velocity of -V to simulate the TSHD sailing. Pressure outlet is also about 2LPP from stern, which will not influence the flow field behind the stern and appendages.

In all cases, free surface are considered, so VOF, volume of fluid method, is applied to the tests simulation. For all the experiments are PMM, the TSHD is fixed in the virtual towing tank, and trim, heave and sinkage are not taken into account. In order to solve the viscous flow with a free surface, RANS models for turbulence based on k-ω model are employed [9].

5 RESULTS AND DISCUSSION

5.1 GRID INDEPENDENCE

Firstly, in order to validate the grid independence, grids of different density are applied to simulate the resistance performance at 10kn. According to table.4, the resistance result does not change apparently between densities of 7474218 and 2180269. So the results validate that the grids at 3rd level can satisfy the precision and effectiveness requirements of the following calculations.

Table.4: Resistance at 10Kn with grids of different densities

Grid density	[-]	coarse	medium	dense	More dense
Grid number	[-]	300816	572600	747218	2180269
resistance	[N]	8.656	8.170	8.094	8.006

5.2 STATIC RESISTANCE

The static resistance performance of the TSHD at various speeds is calculated based on the background grids and overset around the rudders, neglecting the effect of propellers. Experiments and numerical methods are both utilized.

Table 5: Comparisons of TSHD between the numerical results and the experimental results

V_s [kn]	V_m [m/s]	EFD [N]	CFD [N]	Err. [-]
3.00	0.289	0.999	0.988	-1.1%
5.00	0.386	2.221	2.242	0.9%
9.00	0.868	6.911	6.610	-4.3%
10.00	0.964	8.219	8.094	-1.5%
11.00	1.061	10.220	9.999	-2.2%
12.00	1.157	12.249	12.175	-0.6%
13.00	1.253	14.569	14.741	1.2%

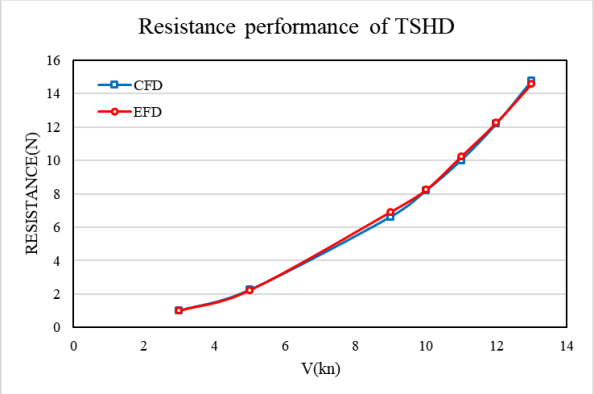

Figure 5: resistance curves of TSHD

As shown as table.5 and Fig.5, the resistance of TSHD improves as the velocity increases. Through comparison between CFD and EFD method, errors have been found smaller than 5%. EFD accord with CFD results well. The results indicate that the EFD method and overset method can predict the resistance performance of TSHD, and the grid can support the numerical simulation effectively. The time history of TSHD resistance at 13kn shows a good convergence, and cases under other working conditions are similar to it (seen in Fig.6).

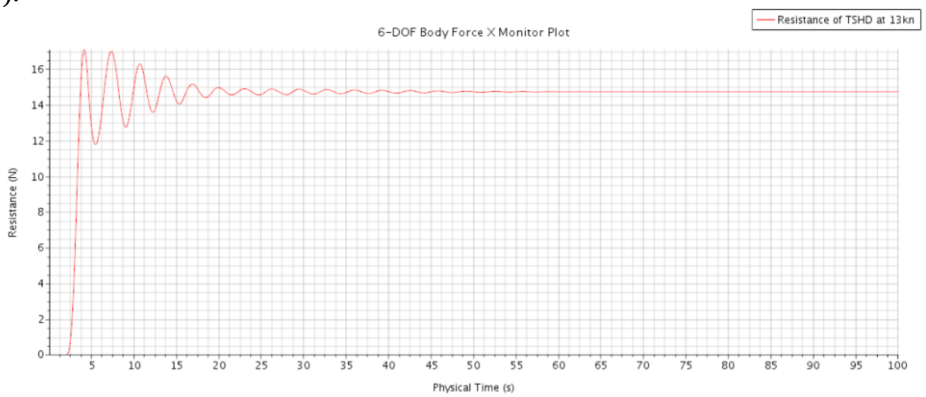

Figure 6: Time history of resistance at 13kn

5.3 SELF-PROPULSION PERFORMANCE

Finally, the compulsory self-propelled method is employed in the self-propelled test both numerically and experimentally. In the tests, overset method will be used to simulate the rotation of the propellers. Overset grids around propellers are added to the simulations. The regions around propellers including oversets surrounding the propellers are rotated at a certain rpm to simulate the self-propulsion tests. Cases for the self-propulsion performance are listed in table.6:

Table 6: Cases for self-propulsion performance study

Working condition	appendage	N_m[rpm]			
5kn	Original propeller	540	780	900	1020
5kn	Ducted-propeller	540	720	900	1020
10kn	Original propeller	840	900	960	1020
10kn	Ducted-propeller	780	840	900	960

According to table.6, numerical simulations are carried out to simulate the self-propelled tests. The experiments are also conducted to verify the method. Forces on TSHD equipped with the ducted-propeller rotating at different RPMs are shown in the fig.7. Performances and forces at self-propulsion point calculated numerically and experimentally at 2 working conditions are shown in table.6. The compulsory force at self-propulsion points under different working conditions are calculated according to the static resistance results, 0.826N at 5kn and 2.667N at 10kn.

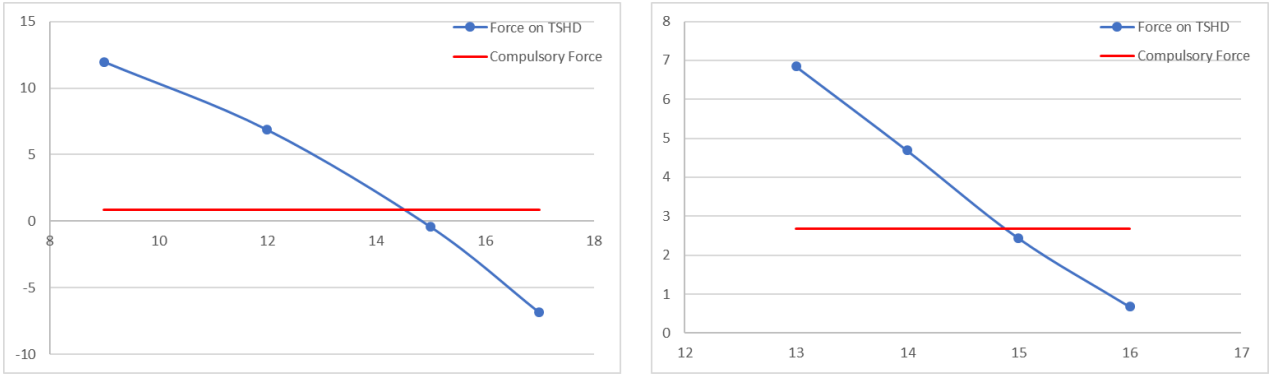

(a) 10Kn (b) 5Kn

Figure 7: Forces on TSHD at different velocities

Table.7: CFD and EFD results of self-propulsion tests with ducted-propellers at self-propulsion point

		10kn			5kn		
Force		CFD	EFD	Err.	CFD	EFD	Err.
Thrust	[N]	3.562	3.623	-1.68%	9.520	9.97	-3.9%
Torque	[N*m]	0.076	0.064	18.75%	0.126	0.110	14.5%
N_m	[rpm]	898.62	885.06	1.53%	909.48	942.66	3.47%

Table.7 shows a good accordance in thrust and rpm between CFD and EFD method, but there is a difference in torque between CFD and EFD method, but the tendency of torque with CFD method is similar to EFD.

The same settings are also applied to simulate the tests with original propellers. Force on the TSHD self-propulsion of TSHD equipped with original propellers are shown in table.8:

Table.8: CFD results of self-propulsion tests with original propellers at self-propulsion point

Force		10kn	5kn
Thrust	[N]	3.638	9.782
Torque	[N·m]	0.084	0.145
N_m	[rpm]	901.32	997.8

According to the results, wake fraction, thrust deduction, power and other coefficients of real ship and propellers can be calculated (seen in table.9). Thrust deduction are considered the same between model scale and real ship scale. Wake fraction is modified through empirical equation [3].

$$w_s = t + (w_m - t) \times \frac{C_{fs}}{C_{fm}} - 0.03 \tag{3}$$

Table.9: wake fraction, thrust deduction power and other coefficients of real ship

Working condition	appendage	t [-]	w_s [-]	N_s[rpm]	QPC [%]	P_D [kW]
5kn	Original propeller	0.125	0.095	286.3	26.6	4116.2
5kn	Ducted-propeller	0.101	0.159	239.2	35.4	3091.0
10kn	Original propeller	0.201	0.143	211.7	38.2	1849.8
10kn	Ducted-propeller	0.243	0.227	201.0	40.0	1771.3

Through self-propulsion simulation under different conditions, propeller performances are found distinct between 2 types of propellers.

From table.8, thrust deduction of original propeller is similar to the ducted-one under both working conditions. Thrust deduction of the original one is higher at 5kn and lower at 10kn. Wake fraction of ducted-propeller is much higher than the origin one under both conditions, which means rate of advance of ducted propellers is smaller than the original one. According to the table.8, the rotating speed and total efficiency of original propellers are much higher which means that the energy consumption of ducted propeller is much smaller, and ducted-propeller has a much better performance than the original one.

Fig.8 shows the velocity field behind 2 propellers respectively and Fig.9 shows the pressure distribution on the different propeller surfaces.

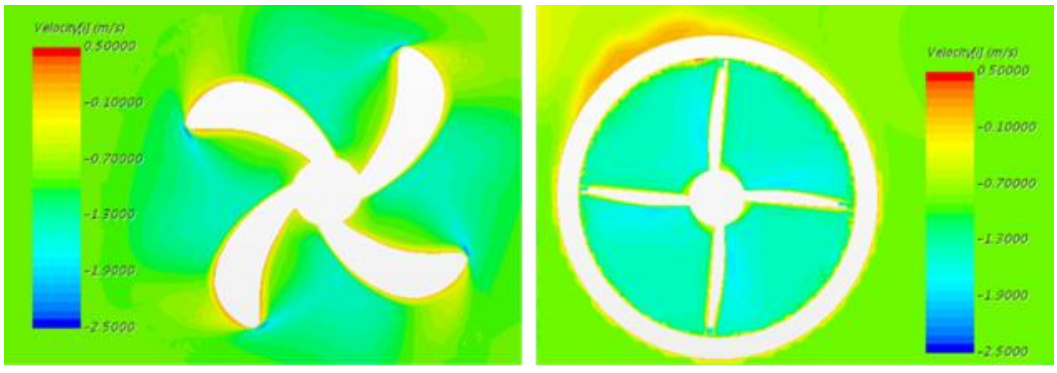

(a) (b)

Fig.8 velocity field at propeller disk at 900 rpm: (a) original propeller
(b) ducted propeller

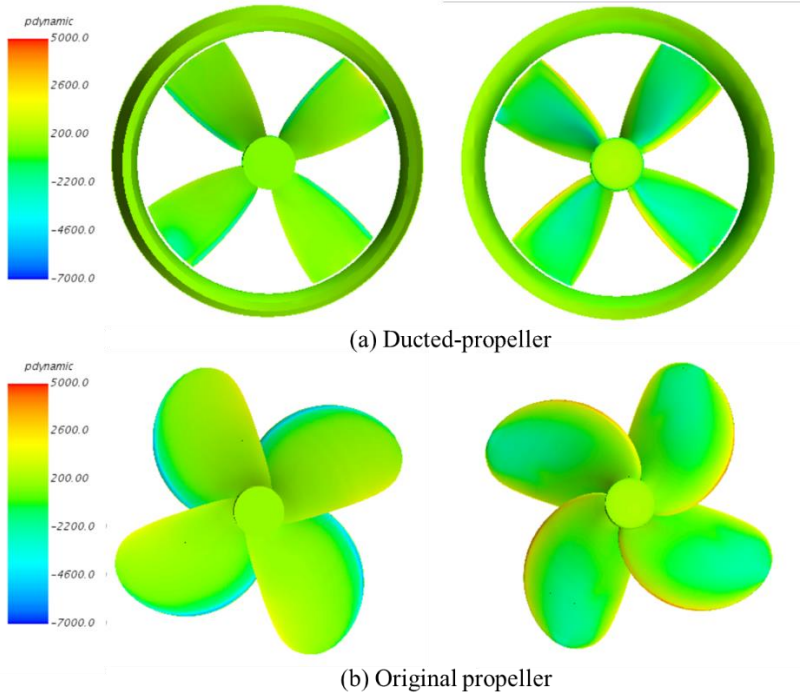

Fig.9 pressure distribution on propeller surface at 900rpm

According to fig.8 and fig.9, velocity at the original-propeller disk occupies a larger area than ducted-propeller. So flow field of ducted-propeller is more concentrated than the original one, which causes a higher wake fraction. The ducts influence the velocity and cause the backflow, which decreases the velocity around the ducted-propeller, and produce a higher pressure difference on the propeller surface, which provides a higher thrust.

The flow conducted by 2 kinds of propellers also influence the resistance of the hull and rudders differently. Fig.10 and fig.11 show pressure distribution on the bare hull and rudders of TSHD under 2 working conditions.

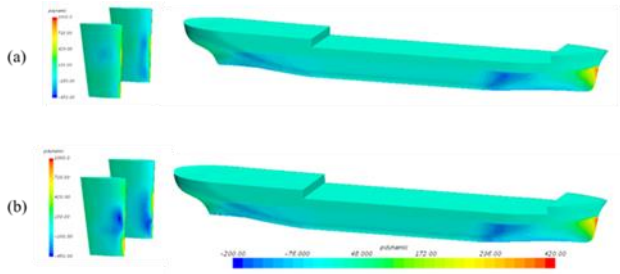

Fig.10 TSHD's pressure distribution at 10kn: (a) original propeller
(b) ducted propeller

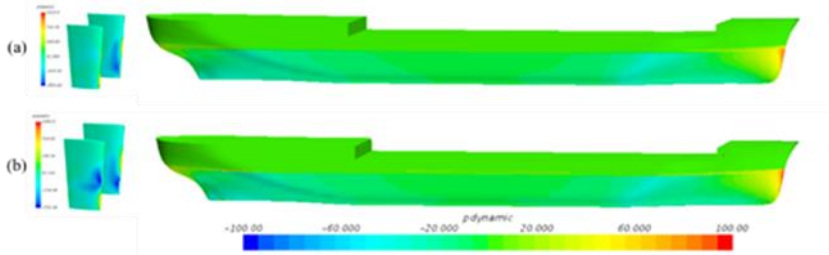

Fig.11 TSHD's pressure distribution at 5kn: (a) original propeller
(b) ducted propeller

Form fig.8 and fig.9, pressure distributions on the hull surface are similar at the bow area, while distributions on rudder and stern surfaces are different. The flow conducted by the ducted-propellers, which is more concentrated, causes a bigger low-pressure area and a higher resistance performance.

6 CONCLUSION AND PERSPECTIVE

In the present study, CFD technology and experiment method are employed to calculate the resistance performance of TSHD. Self-propulsion performances of TSHD equipped with different propellers under various working conditions are also calculated and predicted. The model-propellers are used instead of body force, which can show the feature of flow field conducted by ducted-propellers.

When calculating resistance performance of TSHD, the computational results are consistent with the test results. The error is all below 5%. The well agreements between numerical and experimental results show the grid and modelling of TSHD is credible.

When calculating self-propulsion performances of TSHD with 2 different propellers, numerical results accord with the tests results basically, and error in torque may be produced by the grid density and computational accuracy. Finally, the comparison between 2 propellers shows that the ducted-propeller is better than the original propeller. The efficiency of ducted-propeller is 1.8% higher at 10kn and 8.8% higher at 5kn. The power ducted propeller needed is much lower than that of original one.

Development of meshing improvement is necessary for future work. For the pressure distribution can be obtained from numerical method, it will be feasible to compare rudder effects at various rudder angles and drift angles, which can provide a reasonable solution for rudder optimization or molded lines modification.

7 REFERENCE

[1] Kik, A. (2003). Design Optimization of Trailing Suction Hopper Dredgers How to achieve the maximum result with your investment. *China International Dredging Congress & Exhibition*.

[2] Shi, W. (2013). Dynamics of Energy System Behaviour and Emissions of Trailing Suction Hopper Dredgers:. *International Conference on Mechatronic Sciences, Electric Engineering & Computer*. IEEE.

[3] Choi, J. E. , Min, K. S. , Kim, J. H. , Lee, S. B. , & Seo, H. W. (2010). Resistance and propulsion characteristics of various commercial ships based on cfd results. *Ocean Engineering, 37*(7), 549-566.

[4] Seo, J. H. , Seol, D. M. , Lee, J. H. , & Rhee, S. H.. (2010). Flexible cfd meshing strategy for prediction of ship resistance and propulsion performance. *International Journal of Naval Architecture and Ocean Engineering, 2*(3), 139---145.

[5] Carrica, P. M. , Ismail, F. , Hyman, M. , Bhushan, S. , & Stern, F. . (2013). Turn and zigzag maneuvers of a surface combatant using a urans approach with dynamic overset grids. Journal of Marine Science and Technology, 18(2).

[6] Mofidi, A. , & Carrica, P. M. (2014). Simulations of zigzag maneuvers for a container ship with direct moving rudder and propeller. Computers & Fluids, 96, 191-203.

[7] Sakamoto, N. , Carrica, P. M. , & Stern, F. (2012). Urans simulations of static and dynamic maneuvering for surface combatant : part 1. verification and validation for forces, moment, and hydrodynamic derivatives. Journal of marine science and technology, 17(4), 422-445.

[8] Ban[1], D. , Basic[1], J. , & Dobrota[2], D. (2017). Split tshd hydrostatic particulars calculation for cargo discharge phase using polynomial rbf. Journal of Marine Science and Application: (16), 158.